

**Final Report for DE-FG07-96ER20255 Project
December, 2004**

**Mechanisms of Heavy Metal Sequestration in Soils:
Plant-Microbe Interactions and Organic Matter Aging**

Principal Investigators: Teresa W.-M. Fan^{1,2,3}, Richard M. Higashi^{2,6}, and David Crowley⁴
with Collaborators Andrew N. Lane^{1,5}, Teresa A. Cassel⁶, and Peter G. Green⁷

¹Dept. of Chemistry, Univ. of Louisville, Louisville

²Center for Health and Environment, Univ. of California, Davis

³Dept. of Land, Air and Water Resources, Univ. of California, Davis

⁴Dept. of Soil and Environmental Sciences, Univ. of California, Riverside

⁵J.G. Brown Cancer Center, Univ. of Louisville, Louisville

⁶Crocker Nuclear Laboratory, Univ. of California, Davis

⁷Dept. of Civil and Environmental Engineering, Univ. of California, Davis

National Environmental Technology Testing System (NETTS) sites assistance provided by:
Mr. Donald Gronstal, Mr. Albert Calise, and Mr. Timothy Chapman at McClellan AFRPA
Dr. Robin Brigmon at DOE Savannah River Site

I. Executive Summary

For stabilization of heavy metals at contaminated sites, the three way interaction among soil organic matter (OM)-microbes-plants, and their effect on heavy metal binding is critically important for long-term sustainability, a factor that is poorly understood at the molecular level. Using a soil ageing system, the humification of plant matter such as wheat straw was probed along with the effect on microbial community on soil from the former McClellan Air Force Base. In addition, using forest soil from the DOE Savannah River Site, and bare sump soil from the former McClellan Air Force Base, we ¹³C-labeled the soil humates (HS) in order to investigate the turnover of seven organic amendments (cellulose, wheat straw, pine shavings, chitin, bone meal, lignosulfonate, and sugared lignosulfonate) in relation to heavy metal ion leaching in longer-term (up to 299 days) soil column experiments. The labeled molecular substructures in HS were examined by multinuclear 2-D NMR and pyrolysis GC-MS while the element profile in the leachates was analyzed by ICP-MS. The studies revealed that peptidic and polysaccharidic structures were highly enriched, which suggests their microbial origin. Cd(II) leaching was significantly attenuated with humification of lignocellulosic materials. Examination of ¹³C turnovers of HS substructures have suggested that the biogeochemical turnover itself – not the abundance – is important to reduced metal leaching. In practical terms, these results suggest to us that, in order to reduce leaching and stabilize metals in soil, the starting materials (amendments, natural plant litter, etc.) may need to elicit biogeochemical changes that promote within the HS, the turnover of PS and abundance plus turnover of lignic OM. Alternatively, “poor” starting materials with otherwise desirable characteristics, might stabilize metals if the biogeochemistry (vegetation, microbial community, etc.) of the site can be managed or coerced to promote turnover of PS and lignic OM into HS.

II. Introduction

The myriad of human activities including strategic and energy development at various DOE installations have resulted in the contamination of soils and waterways that can seriously threaten human and ecosystem health. Development of efficacious and economical remediation technologies is needed to ameliorate these immensely costly problems. Bioremediation (both plant and microbe-based) has promising potential to meet this demand but still requires advances in fundamental knowledge. For bioremediation of heavy metals, the three-way interaction of plant root, microbial community, and soil organic matter (SOM)¹ in the rhizosphere is critically important for long-term sustainability but often underconsidered. Particularly urgent is the need to understand processes that lead to metal ion stabilization in soils, which is crucial to all of the goals of bioremediation: removal, stabilization, and transformation.

This work builds on the knowledge and tools that we have generated relating root exudation and metabolism (Fan, et al. 1997; Fan, et al. 2000; Fan, et al. 2001; Shenker, et al. 2001) as well as SOM structures (Higashi, et al. 1998; Fan, et al. 2000) to metal mobilization and accumulation. Both root exudates and SOM (humic substances or HS in particular) are the major organic players in metal ion interactions in soils and sediments. We found that root-exudated phytosiderophores (i.e. mugineic acids, known to be involved in transition metal uptake into plants) (Clark, et al. 1988; Marschner 1995) were not associated with the accumulation of heavy metals such as Cd.

On the other hand, isolated soil HS appeared to facilitate metal bioaccumulation while alleviating Cd-induced growth reduction in wheat plants (Baraud, et al. manuscript accepted). The ability of HS to protect plants from toxic effects of excess metals has also been reported previously (Strickland, et al. 1979; Kinnersley 1993). The above two effects are seemingly contradictory and are difficult to explain based on the strong affinity of HS towards metal ions and their presumed inability to penetrate plant cell membranes. Due to the complex nature of HS, it is conceivable that different parts of the HS structure may mediate different functions regarding metal ion mobilization or immobilization. To make matters even more complex is the fact that different HS substructures have varying turnover rates by microbes, possibly due to such factors as variation in microbial community, physical or chemical protection by soil matrix, and/or innate biochemical stability. Strongly bound metal ions can be released from HS if the interacting HS substructures are degraded by microbes, which makes HS turnover a crucial factor in the stability of HS-metal complexes. Therefore, to gain a mechanistic understanding of HS functions in metal ion bioavailability, it is most fruitful that the structure basis for metal ion interactions and the associated effect on HS turnover be unraveled.

To investigate HS structure in relation to metal ion binding, we prepared ¹³C-labeled soils from a DOE Savannah River Site (SRS) forested site, and the former McClellan Air Force Base (MAFB) bare soil sump, which were in turn employed in soil column experiments where different organic amendments were humified for up to one year. The labeled HS in these soils was then used as turnover indicators for the humification process of various organic amendments. In this report, we describe results of ¹³C labeled HS structure characterization and effect of humification on metal ion leaching properties.

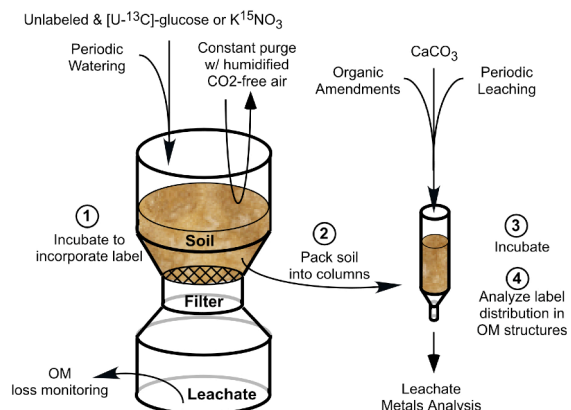
The results are in three phases: (a) Development and initial studies, using MAFB soil; (b) labeled soil studies using SRS forest soil and amendments; (c) labeled soil studies using MAFB sump soil and amendments.

III. Materials and Methods

III.A. Soils

“SRS” soil was collected by Dr. Robin Brigmon from two horizons (surface and 0.5 m depth) in an uncontaminated area near the Tim’s Branch stream system at the DOE SRS site, and stored at 4 °C in the dark until use. Our interest in working with this type of soil stems from the fact that Tim’s Branch, a second order stream system flowing into a tributary of the Savannah River, experienced large influxes of depleted and natural uranium (U), nickel (Ni), and aluminum (Al) as well as other metals. Tim’s Branch soils and vegetation have had a strong impact on the deposition of metals and metal-laden sediments. The SRS soil was processed to 1-2 mm size particles by hand grinding and sieving to remove rocks and non-soil materials and was stored in sealed bags at 4°C until use.

“McClellan” soil was collected with the help of Mr. Al Calise and Mr. Don Gronstal (Air Force Real Property Agency) from a Cd-contaminated area (PRL 60) in the former McClellan Air Force Base, Sacramento, CA. The soil was regularly flooded naturally, and this sump has additionally been contaminated with Pb, Cr, Ba, Ni, Cu, Ag, and petroleum hydrocarbons. It is relatively low in SOM presumably due to the lack of vegetation input. The soil was processed to 1-2 mm size particles by hand grinding and sieving to remove rocks and non-soil materials. The % moisture (27.4%) was determined from the soil weight loss after lyophilization. The processed soil was stored in sealed bags at 4°C until use.



Scheme A. Setup for stable isotope labeling and ageing of soil organic matter. The filter apparatus on the left was used to prepared soil labeled with ^{13}C -U-glucose, ^{15}N -nitrate, or ^{13}C -U-glucose+ ^{15}N -nitrate. The upper soil compartment was aerated with humidified CO_2 -free air (achieved by passing air through KOH pellet). Preiodic irrigation of soil with DI water was performed to maintain soil humidity. The volume of water was controlled to minimize loss of labeled precursors via leaching. The column on the right was used for soil ageing experiments.

III.B. Ageing and Labeling of Soils

A soil ageing experimental system capable of stable operation for several months (see left half of Scheme A) was developed, then used for analytical method development and for an initial survey of the effect of organic amendments on soil OM transformation. For the development phase, we used the PRL60 soil from MAFB. This system was then used to produce ^{13}C -labeled SRS soils by incubating the soils with $[\text{U}-^{13}\text{C}]$ -glucose for 34 weeks at 25 °C. In Scheme A, the left setup for labeling soil is a polysulfone, airtight, Buchner vacuum filtration system (Nalgene, Inc.), while the right setup for humification of organic amendments consists of parts for a polypropylene solid-phase extraction device (Alltech, Inc., Deerfield, IL, USA). $[\text{U}-^{13}\text{C}]$ -glucose together with KNO_3 dissolved in deionized H_2O was added to each pot to double the percent nitrogen in the soil and to increase the existing soil carbon by 10-33%. These additions were performed at week 0, 5, 10, and 23. Ageing of labeled components was initiated with 100 grams each of field moist soil in four pots, two each with the surface and subsurface soils. Soil pots

were irrigated monthly with a nitrogen free micronutrient solution, adapted from Bundy and Meisinger (1994), containing 7mM CaSO₄, 2mM MgSO₄, and 5 mM KH₂PO₄ at pH = 6.0 applied under vacuum for approximately 30 minutes. Leachates were collected from the receivers, freeze-dried, and analyzed for loss of labeled supplements. The first four irrigations used 25 mL of solution, and the subsequent six were made with 15 mL of a 2X concentrated solution to minimize leaching of the labeled supplements.

For labeling of the PRL60 soils, a similar procedure was used as for the SRS soil experiment. It was incubated with uniformly ¹³C-labeled glucose (3 aliquots of 2.5 g per 200 g soil) for 8 months with weekly deionized water irrigation and bimonthly label supplement (see Scheme A for setup). Parallel treatments with unlabeled glucose were also performed.

III.C. Cd-contaminated Wheat Roots and Amendments

Wheat plants were grown in a Cd-spiked hydroponic media to generate Cd-bioaccumulated wheat root material (Fan, et al. 2001). This material was added to the ¹³C and ¹⁵N-labeled SRS soils along with five different organic amendments: cellulose, wheat straw, pine shavings, chitin, and bone meal). Duplicate columns were prepared for each amendment. The columns were kept at 25°C and irrigated regularly with macronutrients (i.e. Ca, Mg, P) to maintain microbial activities. Ageing was conducted for 299 days.

For the PRL60 soils, 20 g each of the ground soil was amended with 1% (w/w) each of cellulose (Cel, Sigma Chemicals, St. Louis, MO), wheat straw (WS), pine shavings (PS), or 0.25-1.5% of lignosulfonate (LS) or sugared LS (SLS) (Aldrich Chemicals). Initial ageing was conducted without CaCO₃, which resulted in soil acidification. Subsequent ageing experiments were performed with 0.5% (w/w) CaCO₃ to maintain soil pH. Also included were a blank (with no amendment) and a CaCO₃ only treatment. CaCO₃ and organic amendments as powder form were mixed thoroughly with the soil before packing into a 25 ml column. The column bottom was fitted with a glass frit and a 0.45 µm cellulose membrane to prevent fine soil particles from leaching. An alternative method for LS and SLS application were done by dripping LS or SLS (40 mg/ml) dissolved in deionized water (1.25 ml) onto the soil column. For labeled experiments, 14-15 g each of the amended soil was used. The moisture of all soil columns were adjusted to about 33% before incubation at 25°C in a humidified environmental chamber. The columns were irrigated weekly with deionized water. Soil leachates were collected weekly to monthly by passing 1 ml of deionized water through columns and centrifuging at 329 x g for 3 min. Ageing was conducted for 4-7 months, much shorter than for the SRS soils due to the ending date of this project.

III.D. Microbial Communities

Microbial community was examined by amplifying bacterial 16S rDNA using polymerase chain reaction, followed by density gradient gel electrophoresis (DGGE). For clarity, more detail on these approaches are described alongside the results below in Sections IV.A and IV.B.3.

III.E. Leachate and soil analyses

Soil leachates were analyzed for pH and a broad spectrum of elements by ICP-MS. The elements routinely quantified included Li, Be, Na, Mg, Al, K, Ca, V, Cr, Mn, Fe, Co, Ni, Zn, Cu, Ga, As, Se, Rb, Sr, Ag, Cd, Cs, Ba, Tl, Pb, and U. The aged soils were lyophilized, ground to 250 µm size, and extracted with 0.25 M NaOH for mobile HS (mHS), acidified to remove Ca,

and reextracted with 0.25 M NaOH for calcified HS (CaHS) following our previous procedure (Fan, et al. 2000). Both HS fractions were treated with chelator Tiron to remove exchangeable cations, washed 3 times with 0.1 N HCl, and adjusted to pH 6 before lyophilization in D₂O (1). The isolated HS was then subjected to multinuclear 2-D NMR and pyrolysis GC-MS analysis, as described previously (Olk, et al. 1995; Fan, et al. 2000) and outlined below.

III.E.1. 3-D Fluorescence Analysis: The lyophilized mHS was dissolved in DI water at 0.6-1 mg/ml in the absence or presence of various Cd concentrations before fluorescence measurement using a Safire UV-Vis/fluorescence scanning microplate reader (Tecan) or a thermostatted LS55 scanning spectrofluorimeter (Perkin Elmer). The excitation and emission scan ranges were 230-490 and 270-700 nm, respectively. Contour plots of the 3-D data were made to discern spectral changes induced by Cd additions.

III.E.2. NMR Analysis: The mHS was dissolved in D₂O and analyzed on two Varian Inova NMR spectrometers (Varian, Inc., Palo Alto, CA) at 14.1 T and 18.8 T. The NMR experiments conducted included 1-D ¹H NMR, 2-D ¹H TOCSY (total correlation spectroscopy), 2-D ¹H-¹³C HSQC (heteronuclear single quantum correlation spectroscopy), and ¹H-¹⁵N HSQC, as described previously (Fan et al., 2000) to assign labeled substructures and to compare the label abundance. Two additional 2-D experiments (¹H-¹³C HSQC-TOCSY and HCCH-TOCSY) were performed to verify the assignment of ¹³C labeled carbons including those that were consecutively labeled. The NMR analysis of mHS was complemented with pyrolysis-GC-MS (PyGC-MS) analysis, which was also conducted for the whole soil and CaHS.

III.E.3 Pyrolysis-GCMS Analysis: The procedure and instruments for pyro-GCMS were analogous to that described previously (Fan et al., 2000), this time using a Frontier Labs (Koriyama, Japan) Autoshot AS1020E with PY-2020i pyrolyzer interfaced to an Agilent (Palo Alto, CA, USA) 5890 Series II gas chromatograph outfitted with a Frontier Labs UA-5 steel-clad fused silica column of 0.25mm i.d. x 30m length, 0.25µm diphenyldimethylpolysiloxane coating. This system was interfaced to an Agilent 5971A MSD mass spectrometer. Briefly stated, to analyze samples, a sample cup containing 10 mg of soil or 1mg of HS was dropped into a 550°C furnace under a He stream. This caused thermolysis of chemical bonds according to their relative strengths, which generated volatile products. The products were swept by the He stream into the column which resulted in sequential elution of the volatile products. These chemicals eluting from the column were examined by on-line mass-spectral (MS) detection; the identity of many fragments are considered traceable to the parent structural class from which they arose (e.g. Schultz et al., 1999).

Analysis of pyro-GCMS data sets consisted of comparison of chromatographic peaks to available standards for thermolytic products, using structural matching with the aid of a 78,000-compound NIST/NIH/EPA mass spectral library. Peaks associated with a given structural class (lignins, peptides, polysaccharides) were pooled to obtain a net response which was a single numerical peak area value, using our previous approach (Schultz et al., 1999). These responses were compared with pyro-GCMS analyses of purified components such as microcrystalline cellulose (Sigma), inulin AT, and bovine serum albumin (Sigma). Standard paper filters (Whatman #451) were found to be highly reproducible and was analyzed periodically to assess changes in instrument analytical response; changes were negligible (<3%) for the duration of the

analyses, therefore the data warranted no instrument response correction. Data analysis for isotopic enrichment is described with the results.

IV. Results and Discussion

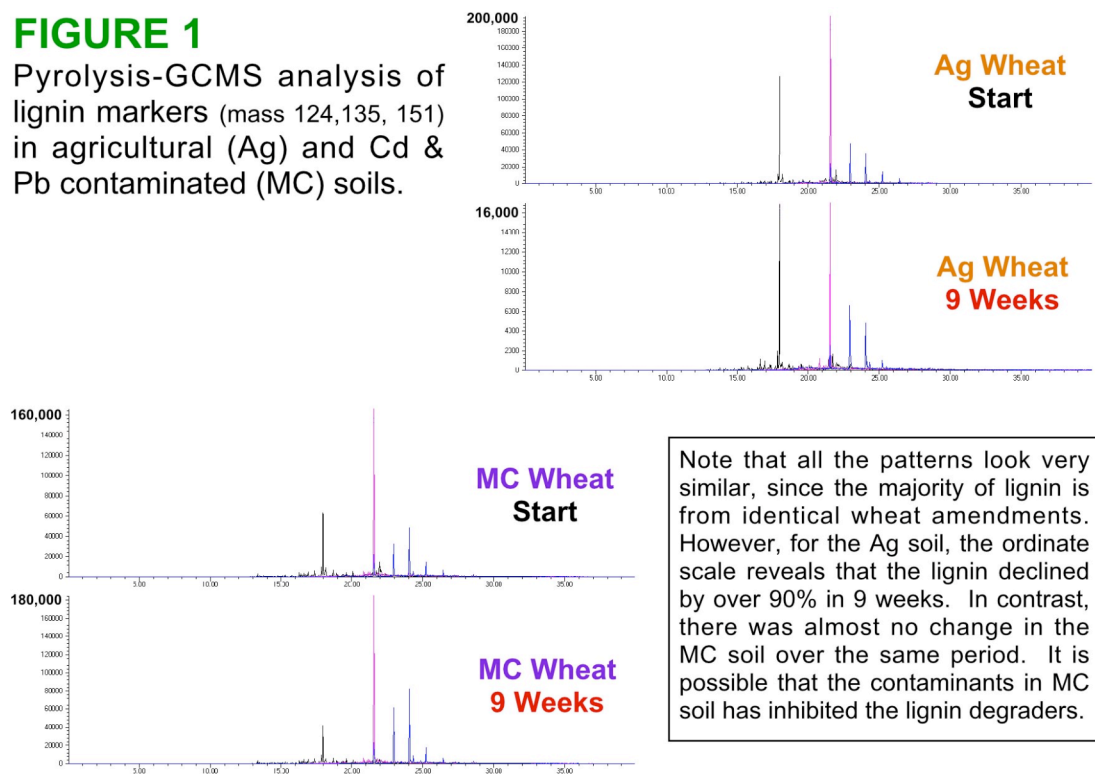
As stated in the Introduction, the results are reported in three phases: (a) Development and initial studies, using MAFB soil; (b) labeled soil studies using SRS forest soil and amendments; (c) labeled soil studies using MAFB sump soil and amendments.

IV.A. Development and Initial Studies

Figure 1 shows organic matter analysis of an agricultural soil (Ag) from the Long-Term Agricultural Research Site (LTRAS) low in Cd and Pb concentrations and, a Cd and Pb contaminated soil (MC) from the former McClellan Air Force Base (MAFB), both of which were amended with wheat straw. The high lignin degradation rate observed for the Ag soil indicates that the microbes were active and is consistent with the adaptation of the microbes to lignin breakdown in agricultural soils. In contrast, the subsurface soil from McClellan shows little lignin degradation, which suggests the lack of lignin-degrading microbes or adaptation in this soil. The Pb and Cd contamination in the MC soil could in part underlie this lack of lignin degradation.

FIGURE 1

Pyrolysis-GCMS analysis of lignin markers (mass 124, 135, 151) in agricultural (Ag) and Cd & Pb contaminated (MC) soils.

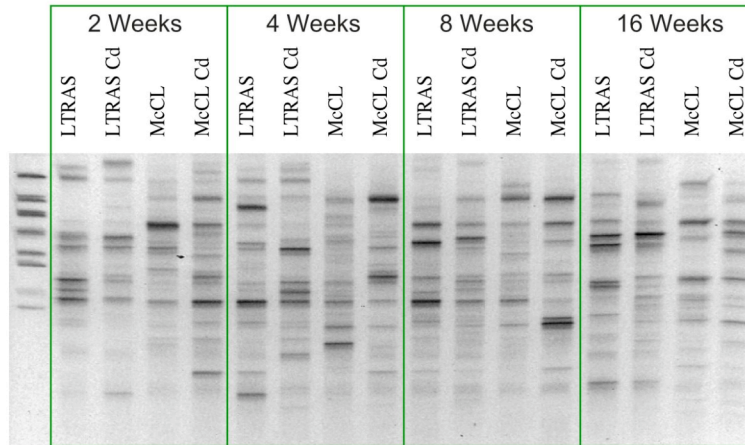


Using the 16S rDNA typing approach (see section IV.B.3), the time course change in microbial profiles for both Ag and MC soils was acquired, as shown in Figure 2. It is clear that microbial profile differed between the Ag (or LTRAS) and MC (or McCL) soils both initially and after 16 weeks of incubation. Both sets of profiles also changed with time and with the presence of Cd (derived from Cd-loaded wheat roots). A cluster analysis of the microbial profiles, as shown in Figure 3, reveals that the Cd impact was more pronounced in the MC than in the Ag soil and this effect was greatest during early decomposition of wheat roots. This observation may be related to a better Cd adaptation of microbial community in the Cd-

contaminated MC soil. The presence of Cd may enhance those adapted microbial populations in the early exposure stage. Further sequence analysis of the 16S rDNA isolated from the two soils should help identify the changing microbial populations.

FIGURE 2

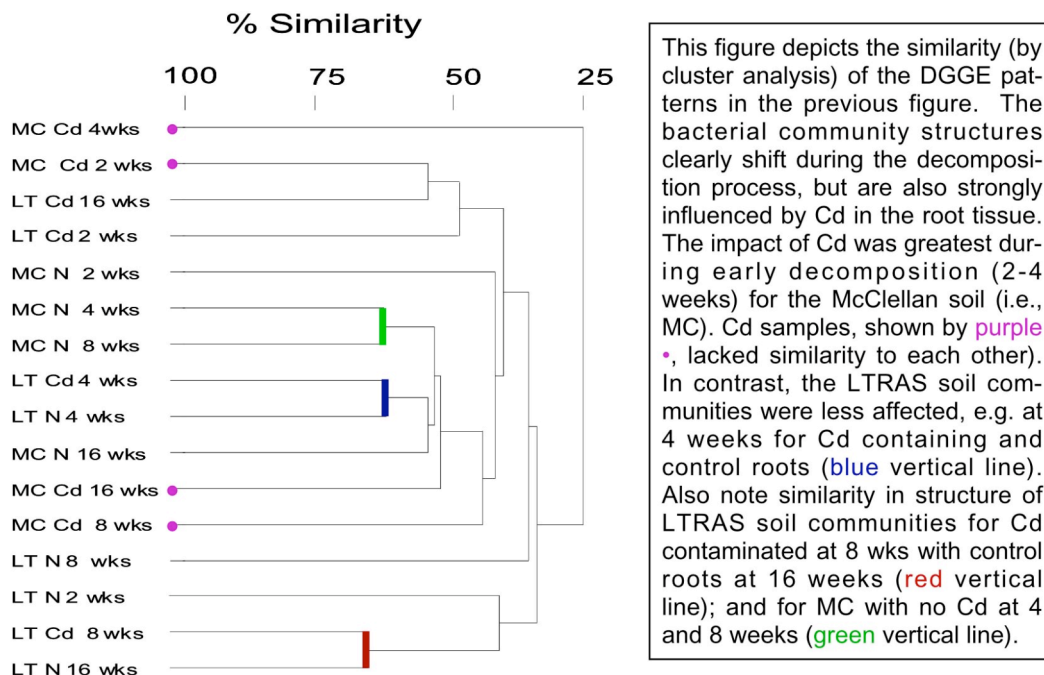
Effect of Cd on bacterial communities associated with decomposing plant roots in agricultural (LTRAS) and Cd-contaminated (McCL) soils.



Bacterial communities are represented by polymerase chain reaction-denaturing gradient gel electrophoresis (PCR-DGGE) of 16S rDNA extracted from decomposing plant roots after 2, 4, 8, and 16 weeks of decomposition. Each band represents a different group or species of bacteria. Changes over time reveal the impact of cadmium on bacterial community species composition during the decomposition process.

FIGURE 3

Similarity (cluster analysis) of the DGGE data in Fig. 2



IV.B. Labeled Soil Studies with SRS Forest Soil and Amendments

IV.B.1. Label incorporation and amendments

Once we were able to introduce ^{13}C label into soil in the preceding section, we turned to SRS forest soil for the experiments. Figure 4 illustrates the 2-D NMR characterization of ^{13}C and ^{15}N -labeled HS isolated from the SRS soil at the end of the labeling period, but prior to the 299-day incubation with organic amendments. The ^1H - ^{13}C HSQC analysis (Fig. 4A) revealed covalent linkages of enriched carbons to protons, from which labeled functional group of certain HS substructures can be deduced. It is interesting to note that the ^{13}C enrichment was high in the aliphatic carbons from peptide and ring carbons from carbohydrate substructures of HS. This labeling pattern is consistent with microbial turnover of ^{13}C -glucose and incorporation of microbial biomass into HS. In a parallel experiment, the ^{15}N enrichment in peptidic backbone and side chains as illustrated in the ^1H - ^{15}N HSQC analysis (Fig. 4B) indicates microbial reduction of the precursor ^{15}N -nitrate, synthesis of proteins, and incorporation of protein residues into HS. These labeled patterns were consistent with the pyrolysis GC-MS analysis (data not shown). Namely, pyrolyzed fragments that are of protein and polysaccharide origins were enriched in ^{13}C and ^{15}N . The finding that these biochemically labile residues persisted in HS suggests that some kind of protection (e.g. physical or chemical) mechanism was operative.

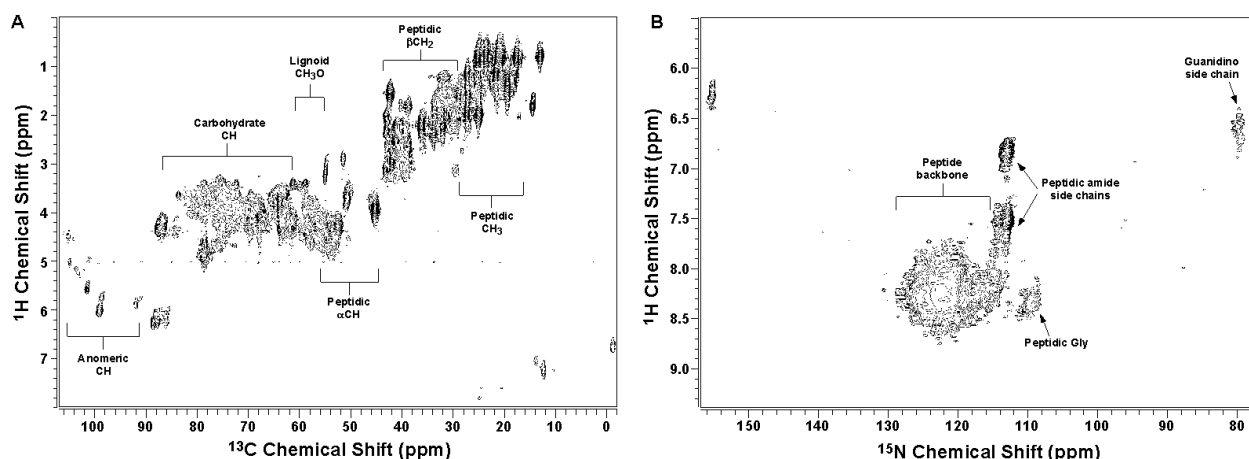
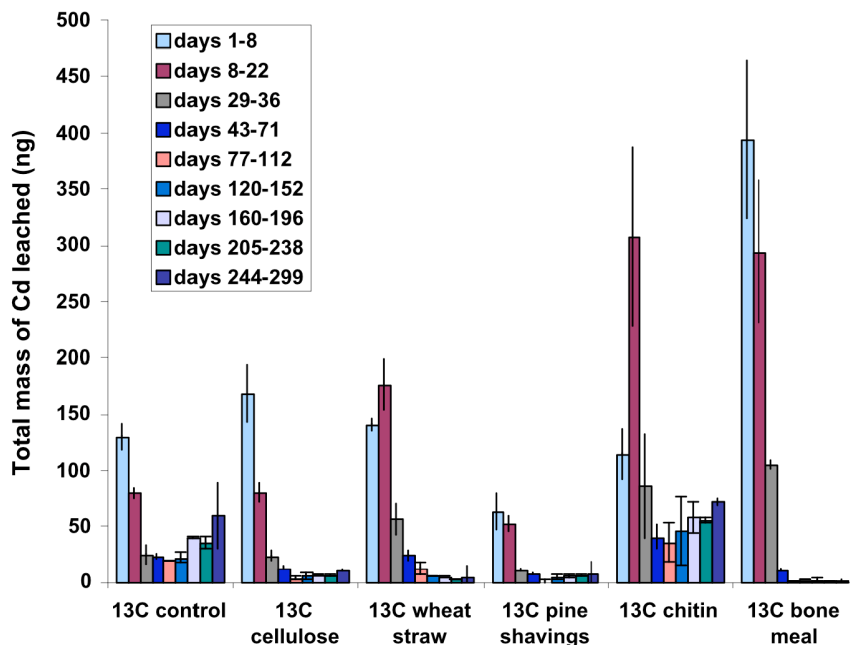


Figure 4. 2-D NMR ^1H - ^{13}C HSQC (A) and ^1H - ^{15}N HSQC (B) analysis of labeled SRS HS.

FIGURE 5

Cd Leached from ^{13}C -Labeled Soil Columns Amended with Cd-Roots



Total Cd mobilized by periodic rinsing of ^{13}C labeled SRS soils spiked with Cd-bioaccumulated wheat root and organic amendments as noted. Initial Cd concentrations averaged 2.4 mg/kg (range = 1.6-3.4 mg/kg). The chitin and bone meal caused increased Cd leaching initially while pine shavings decreased it significantly. After 299 days of incubation, except for the chitin treatment, all organic amendments led to a reduction in Cd leaching, relative to the control. As expected, Cd experienced most of its loss in the first four leachings (days 1-22). The corresponding ^{15}N labeled experiments behaved similarly. Cd was analyzed by ICP-MS and each value represent an average of duplicate samples.

During the course of incubating the ^{13}C -labeled SRS soils with Cd-loaded wheat roots and different organic amendments, different metal leaching property was observed, as shown in Figure 5. Most notably is that except for the chitin treatment, all organic amendments led to a reduction in Cd leaching after 10 months of incubation. Cd leaching was lowest in pine shaving, followed by cellulose- and wheat straw-amended soils. It is also interesting to note bone meal amendment led to an initially high Cd leaching (up to 22 days of incubation) but dropped to below control level thereafter. A similar but less pronounced leaching trend was observed for Cu (data not shown).

IV.B.2. Chemical Studies

For stabilization of heavy metals at contaminated sites, the unavoidable biogeochemistry of HS – not just the static properties of HS – in relation to heavy metal binding is critically important for long-term sustainability, a factor that is poorly understood at the molecular level. Using a soil isotopic labeling system to produce material for soil column experiments described above, the humification process in relation to metal ion mobility was investigated. The soil HS was labeled with ^{13}C using ^{13}C -glucose as the precursor, progress of which was monitored by pyro-GC-MS. Figure 6 illustrates the principle of this analysis. We found that pyrolyzed fragments that are of protein and polysaccharidic origins were highly enriched in ^{13}C . In the example shown in Figure 6, there appears to be primarily two major pools of peptidic structures: non-labeled, and fully labeled. The non-labeled pool, persisting after 34 weeks of incubation with ^{13}C glucose, apparently represents a “recalcitrant” pool of peptidic material in soil, consistent with previous findings (e.g. Fan et al., 2000) and present work on this DOE project (Fan et al., 2004; Higashi et al. 2004).

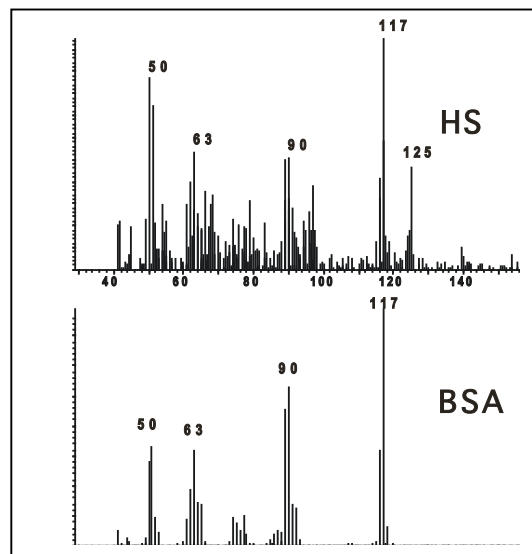
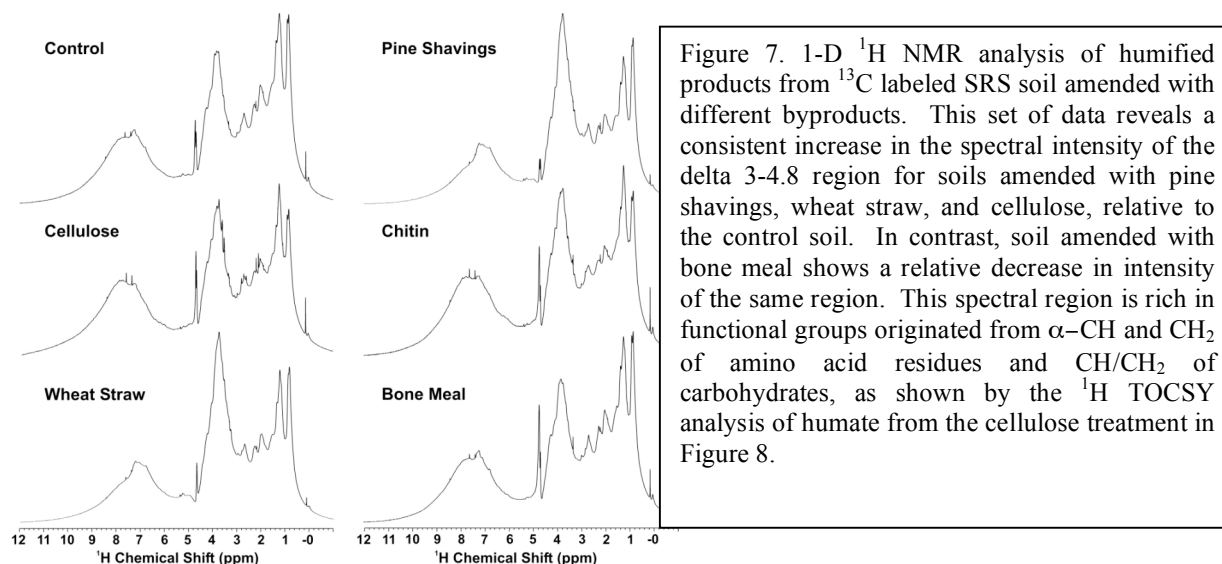


Figure 6. Pyro-GCMS output showing pattern of labeling peptidic groups in the soil incubated with ^{13}C glucose (expt. described in text). Pyro-GCMS thermolyzes peptidic groups to form indole (C_8NH_{10}) with expected all- ^{12}C ion at m/z 117, and the smaller natural abundance ^{13}C ion at m/z 118. Depending on the number of carbons labeled, a distribution of peaks from m/z 117 \rightarrow 125 will be seen for this peptidic marker, with m/z 125 representing a fully ^{13}C -labeled structure. In this particular case, there appears to be primarily two major pools of peptidic structures: non-labeled, and fully labeled. The non-labeled pool, persisting after many months of incubation with ^{13}C glucose, apparently represents a “recalcitrant” pool of peptidic material in soil.

The humified product from some of the aged soils (after 300 days of incubation) have been analyzed by 1-D and 2-D NMR, as shown in Figures 7 and 8. Figure 7 compares the 1-D ^1H NMR spectra of soil humates extracted from soils amended and aged with cellulose, wheat straw, pine shavings, chitin, and bone meals for 300 days. These data reveal the relative increase in the spectral region of δ 3-4.8 for soils amended with pine shavings, wheat straw, and cellulose while a decreased intensity was observed for soil amended with bone meal, as compared with the unamended soil. As described below, this region is largely composed of

resonances arising from amino acids and polysaccharides. It should be noted that the overall spectral appearance for these products is similar to that of humates isolated from natural soils, which suggests that the organic amendments have been adequately humified.



Further 2-D ^1H total correlation spectroscopy (TOCSY) analysis of the humate from the cellulose treatment indicates that this region is rich in αCH and CH_2 of amino acid residues plus CH/CH_2 of polysaccharides (Figure 8). These assignments were made based on the proton covalent connectivity and chemical shift information acquired from the TOCSY spectrum, and is in agreement with the 2-D ^1H - ^{13}C heteronuclear single quantum coherence (HSQC) analysis (data not shown) and assignment of other soil humates (Fan et al., 2000; Fan et al., 2004; Higashi et al., 2004). In addition, based on the chemical shift information from TOCSY and/or HSQC, the amino acid residues are all in peptidic linkages, while the deoxyribose residue are most likely to be originated from nucleic acids. The TOCSY analysis also reveals the abundance of amino acid and saccharidic residues (Figure 8) while the HSQC data indicated the persistence of ^{13}C -enrichment in amino acids including Val, Leu, Ile, Thr, Ala, Asp, and Gly (data not shown). Moreover, the significant presence of Glu/Gln and Pro residues in the humified product, as the case for the starting soil (data not shown), could be attributed to a combination of slow turnover of unlabeled residues and some enrichment, as discussed above.

Complementary pyro-GCMS analysis of the pre- ^{13}C labeled, organic-amended SRS soils provided quantitative information on the abundance of soil OM substructure and their % isotopic enrichment. In Figure 9, these parameters are plotted against total metals leached over 299 days. “Abundance” refers to the total lignic or polysaccharidic (PS) soil OM. “Incorporation” is the total minus the ^{13}C labeled soil OM, that is, displacement of ^{13}C from a given soil OM type, which is an indication of turnover. The analysis involved quantification of each partially-labeled ^{13}C isotopomers for each OM constituent (e.g. a simple case was illustrated in Figure 6). “Isotopomer” analysis is the % ^{13}C enrichment in individual C within a structural fragment. Thus, in the present case, a single pyro-GCMS run took 12 passes of multi-peak data reduction to quantify all the isotopomers for six OM constituents.

As shown in Figure 9 top panel, a higher PS incorporation (closed squares) related well to the reduced Cd leaching, while the PS abundance (open squares) did not. This indicates that the turnover of PS was the controlling factor, not the total amount of PS accumulated in the system. In fact, for the pine shavings, there was very little accumulation of PS over 299 days, while the cellulose treatment actually lost PS (Figure 9, open squares). Yet these two were the most effective in reducing metal leaching (e.g. Figure 5) possibly because of their high turnover (Figure 9, closed squares). The lignic OM (circles) showed a trend similar to that for PS.

For Ni, the results for both PS and lignic OM showed a similar general trend as Cd (Figure 9, middle panel). The typically monovalent Cs behaved somewhat differently from the divalent metals Cd and Ni, in that amendments - including the control - that resulted in any turnover of PS (closed squares) or lignic OM (circles) resulted in lower leaching (Figure 9, bottom panel). As with Cd and Ni, the abundance of the PS OM (open squares) did not relate to Cs leaching. Other soil OM types (e.g. peptidic, alkanic, alkenic) and total soil OM showed little relation to leaching of any elements analyzed in this study (data not shown). However, this does not rule out the involvement of specific residues (e.g. peptidic Glu) in reducing metal leaching since pyro-GCMS data does not distinguish individual amino acids or saccharide monomers.

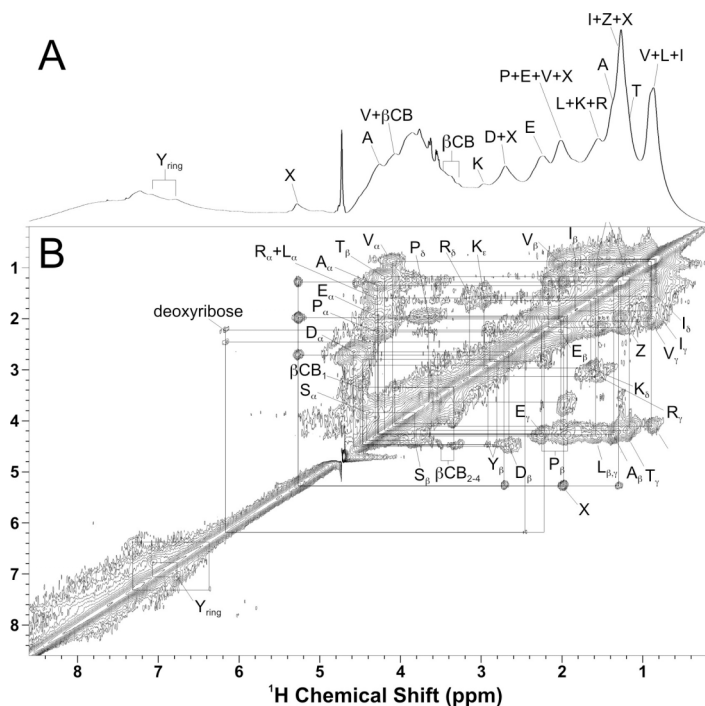


Figure 8. 2-D ^1H TOCSY analysis of soil humate isolated from ^{13}C -labeled SRS soil subsequently aged in cellulose. The spectra shown are 2-D TOCSY (B) along with the 1-D high-resolution ^1H spectra (A). Proton covalent connectivity is traced by rectangular boxes. $\beta\text{-CB}$ represents β -cellobiose while X and Z denote unassigned but abundant structures. Based on the proton connectivity, X should have the structure of $\text{CH}_3\text{-CH}_2\text{-CH}_2\text{-CH-X}$. The letters used for amino acids are as standard biochemical abbreviations: A, alanine; I, isoleucine; L, leucine; V, valine; T, threonine; K, lysine; P, proline; E, glutamate; Q, glutamine; G, glycine; R, arginine; D, aspartate; N, asparagine; S, serine; Y, tyrosine.

Thus, Figure 9 revealed a possible mechanism for the effectiveness of pine shavings and cellulose in reducing Cd, Ni, and Cs leaching, namely, the turnover of PS is important to reduced metal leaching. Figure 9 also reveals that both turnover and abundance of lignic OM may play a role, so that the combination of lignic + PS materials, such as natural plant materials, may be the most efficacious. Yet, this cannot be extrapolated to all plant materials. We found that wheat straw – a lignocellulosic material - caused increased leaching of Cd (Fig. 5) and Ni (data not shown). Figure 9 may be revealing why this was so: for wheat straw, there was no PS incorporation (closed squares, middle panel) for 299 days. Once again, the net loss of PS (open squares, middle panel) over 299 days was not the factor for increased Ni leaching, as cellulose

was effective in reducing Ni leaching but had considerably greater PS loss (Figure 9 middle panel, open square data point at lowest left).

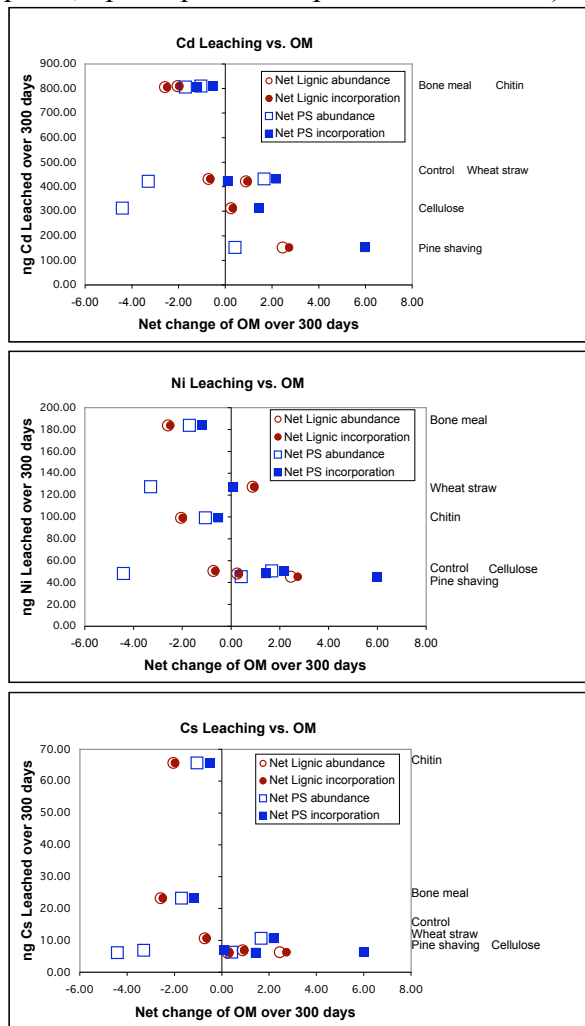


Figure 9. Results of py-GCMS analysis of pre-¹³C labeled, organic amended soils, plotted against data on ordinate from Figure 5 (total metals leached over 299 days). The abscissa is the net change (arbitrary units) of the OM parameter over 300 days. “Abundance” refers to the total lignic or polysaccharidic (PS) OM. “Incorporation” is the displacement of ¹³C from an OM type, effectively constituent turnover. Data on a horizontal line are from a given treatment, listed at right.

In the top panel, note that PS and lignic incorporation (closed symbols) related well to the reduced Cd leaching. However, the PS abundance (open squares) did not. This indicates that the turnover, e.g. via microbial processing, of PS is the controlling factor.

For Ni (middle panel), the results show a similar general trend as Cd, while for Cs (bottom panel), any amount of net turnover (closed squares) related to the same level of reduced leaching; again abundance of PS (open squares) did not relate. Other OM types (e.g. peptidic, alkanic, alkenic) and total OM showed no relation to metal leaching (data not shown). See text for further discussion.

These results suggest to us that, in order to reduce leaching and stabilize metals in soil, the starting materials (amendments, natural plant litter, etc.) may need to elicit biogeochemical changes that promote within the HS, the turnover of PS and abundance plus turnover of lignic OM. Alternatively, “poor” starting materials with otherwise desirable characteristics, might stabilize metals if the biogeochemistry (vegetation, microbial community, etc.) of the site can be managed or coerced to promote turnover of PS and lignic OM into HS.

IV.B.3. Microbial Studies

Responses to cadmium toxicity in bacteria previously have been shown to include the induction of transport systems for elimination of cadmium from the cell by means of a zinc transporter protein, Znt A, that is located in the cell membrane. In *E. coli*, Cd has been shown to cause greater than 30 fold upregulation of this protein as compared to zinc. The ZntA transporter, (a P-type ATPase), is therefore, believed to be a major component of the cadmium stress response. In addition to the zinc transporter, several other stress response systems, including those for heat shock, oxidative stress, the stringent response, and SOS, are also known to be stimulated during Cd stress. However, no previous studies have comprehensively identified Cd-inducible proteins in bacteria, and our knowledge of global gene regulation in response to Cd stress is still very limited. To better understand the toxicity effects of cadmium on bacteria at the gene regulatory level, research conducted here employed an oligonucleotide microarray or gene chip (Affymetrix www.affymetrix.com) to examine gene expression following exposure to cadmium.

In brief, cells of *E. coli* K-12 (MG1655) were grown to the exponential stage and were exposed to 1 ug/ml of Cd (as CdCl₂), after which they were harvested at 5, 15, 25 minutes, and at 20 hr. A Masterpure RNA purification Kit (Epicentre Technologies) was used to isolate total RNA, after which mRNA sequences were enriched by eliminating 16S and 23S rRNA from total purified RNA. The enriched mRNA was fragmented and labeled with biotin, hybridized to the microarrays and scanned using a microarray reader. After two-step filtering of the resulting data, a total of 674 transcripts were determined to be either up or down regulated in response to Cd toxicity (Table 1). These transcripts were subjected both to cluster and classification analysis to characterize the gene functional groups to which they belonged. Of the 674 transcripts that were affected by Cd, 334 genes had known functions, 117 represented open reading frames with unknown functions and 223 corresponded to intergenic regions (Table 1).

Results of this research provided unprecedented insight into bacterial cell responses to cadmium toxicity. Among the different gene functional groups that were affected by cadmium, genes encoding the regulatory and zinc binding proteins are of particular interest with respect to the effects of cadmium on cell physiology. The regulatory genes affected by cadmium are important because transcription factors encoded by these genes directly or indirectly repress or enhance the expression of other genes and operons. Moreover, transcription regulators often network together to cope with specific stimuli. The results showed that in general, genes coding activators for certain stress response were up-regulated, while the gene (*LexA*) regulating the SOS response was repressed (Figure 10). Stress responses activated by cadmium included those for osmotic (*OsmE*, *OmpR*), heat shock (σ^E), and superoxide (*Fur*, *SoxR*) response mechanisms.

The first of these, *OmpR* (regulator) /*EnvZ* (sensor) system regulates an osmosensory pathway in *E. coli*. Following exposure to cadmium, the ratio of *OmpR/EnvZ* expression was approximately 35:1, which suggests that *ompR* was over-expressed, while *envZ* was not induced significantly. The second system mentioned above is the heat shock response system which is regulated by the sigma factor, *rpoE* (σ^E). This sigma factor regulates 43 genes, and is activated in response to misfolded/unfolded outer-membrane proteins. The *rpoE* sigma factor also mediates biosynthesis/transport of lipopolysaccharides, such as *lpxD* (lipidA synthesis), *nlpD* (lipoprotein), *fkpA* (rotamase), and *htrA* (a protease that allows *E. coli* to remain viable at >42⁰C).

These stress responses are consistent with the hypothesis that cadmium caused protein misfolding in both the periplasm and cytoplasm. Still another protein affected by cadmium, *Fur* (*fur*) controls 90 genes in *E. coli*, and is a negative regulator for metal uptake systems, as well as

a positive regulator for detoxification of reactive oxygen species. Transcription of *fur* is activated by SoxR (*soxR*), a regulatory protein in the soxRS regulon for resistance to superoxide. SoxR also regulates *marA* (ST 4) that transcribes over 60 genes and CspA (cold shock protein) (ST 3). All of these responses indicate the far ranging effects of cadmium on cell physiology.

Table 1. Gene expression patterns within gene functional groups in *E. coli* at selected time intervals following exposure to 1 ppm cadmium.

Functional groups	Number of upregulated genes					Number of genes downregulated					
	Total genes	5 min	15 min	25 min	20 hr	Total	5 min	15 min	25 min	20 hr	total
Amino acid biosynthesis and metabolism	130	4	0	1	1	6	8	1	4	5	18
Transport and binding proteins	281	9	1	2	8	20	8	0	4	8	20
Energy metabolism	243	17	0	5	6	28	21	0	7	18	46
Biosynthesis cofactors, prosthetic groups and carriers	103	1	0	2	2	5	1	0	0	1	2
Putative enzymes	251	6	1	3	4	14	3	1	2	2	8
Cell processes (incl. adaptation, protection) phage, transposon, or plasmid	188	8	1	9	9	27	11	2	5	9	27
Translation, post-translational modification	60	1	1	8	5	15	7	0	0	3	10
Putative regulatory proteins	182	5	1	14	4	24	47	1	2	15	65
Regulatory function	133	6	2	1	5	14	2	0	2	2	6
Nucleotide biosynthesis and metabolism	45	1	0	2	3	6	1	0	0	0	1
Other known genes	58	0	0	0	1	1	2	0	0	2	4
Transcription, RNA processing and degradation	26	3	0	1	1	5	1	0	2	2	5
DNA replication, recombination, repair	55	2	0	2	1	5	0	0	0	0	0
Carbon compound catabolism	115	5	0	4	5	14	6	0	0	1	7
Putative transport proteins	129	2	0	0	3	5	1	1	0	0	2
Structural proteins	145	4	0	1	3	8	5	0	3	5	13
Cell structure	42	3	0	1	2	6	0	0	0	0	0
Central intermediary metabolism	182	7	2	4	8	21	6	1	2	5	14
Fatty acid and phospholipid metabolism	88	9	2	3	7	21	10	1	2	8	21
Membrane proteins	48	1	0	2	1	4	4	0	0	3	7
Unknown function ORF	13	0	0	0	0	0	1	0	0	1	2
Intergenic region	NA	43	5	41	32	121	52	2	14	21	89
Total	NA	196	28	175	168	567	302	20	87	189	598

Another regulatory gene that was affected by cadmium was *lexA*, which encodes a global repressor for the SOS regulon, which regulates as many as 30 proteins. When *lexA* is depressed by cadmium, genes encoding functional components of the SOS response including, *recA*, *dnaN*, *dinJ*, and *uvrB* are up-regulated, indicating that the repair pathway activated by Cd is the that used for nucleotide excision repair. This same system typically responds to UV damage and is consistent in suggesting that Cd directly damages DNA.

The effects of cadmium on the zinc-binding proteins was of interest as the replacement of zinc by Cd leads to dysfunctional and structurally altered proteins. In this study, 14 out of the 30 known genes encoding zinc-binding proteins were shown to have differential expression following exposure to cadmium. Of these, the main group affected was that for production of r-protein subunits, which were up-regulated after 20 hours following cadmium exposure. Over-expression of these genes may be explained as compensation for loss of functional zinc-binding proteins due to prior misfolding and dysfunctional proteins that were generated in the presence of cadmium. A full interpretation of these and other responses to cadmium toxicity will be published in the manuscript that will report this research.

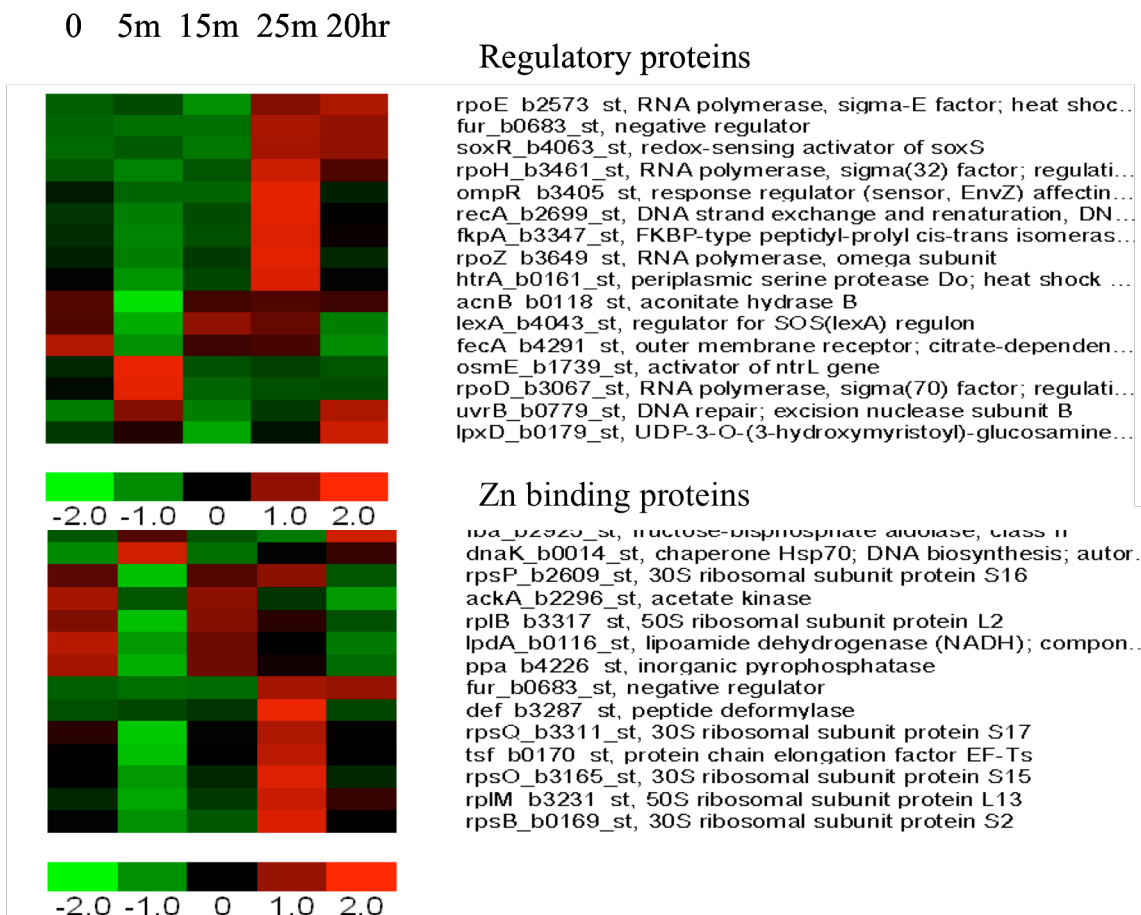


Figure 10. Response patterns for genes encoding regulatory proteins (top) and zinc-binding proteins (bottom) at selected time intervals following exposure to 1 ppm Cd. Bottom color coded bar indicates amount of up or down regulation (log scale) as compared to control cells that were not exposed to cadmium.

IV.C. Labeled Soil Studies with MAFB Sump Soil and Amendments

In the previous section, we described that amending SRS forest soil with plant byproducts of high lignin and cellulose content resulted in low Cd leaching from this soil contaminated with Cd-loaded plant roots. In fact, it was the faster turnover – not the abundance – of lignocellulosic materials that correlated with the reduced metal leaching. This finding prompted the questions whether this mechanism applies to *in situ* metal contaminated soils and whether different lignin byproducts can achieve a similar outcome. These questions were investigated in the next phase by employing several plant byproducts and a Cd-contaminated military base soil that was a bare sump. The byproducts used included:

- Lignosulfonate (LS): a byproduct of pulpmill operation and is rich in modified lignins.
- Wheat straw (WS): a byproduct of agricultural production and is rich in lignocellulose
- Pine shavings (PS): a byproduct of building industries and is rich in lignins
- Cellulose (Cel): a commercial product of pure cellulose

These materials were chosen based on their variation in lignin structures as well as differences in metal leaching outcome observed in the previous phase of research (Higashi et al, in press).

IV.C.1. Ageing/Leaching Experiments of Unlabeled Soils

Initial ageing experiments were conducted to observe the behavior of PRL60 soils from MAFB. These were performed without CaCO_3 amendment, and resulted in a drop of the leachate pH, particularly for the SLS amendment, as shown in Figure 11. The extent of the acidification for LS and SLS was also related to the % amendment and respiratory activity (as measured by CO_2 release, data not shown). These findings suggest that microbial metabolic activities were at least in part responsible for the acidification. It should also be noted that CaCO_3 amendment helped maintain the leachate pH above neutral during the 5-month ageing period.

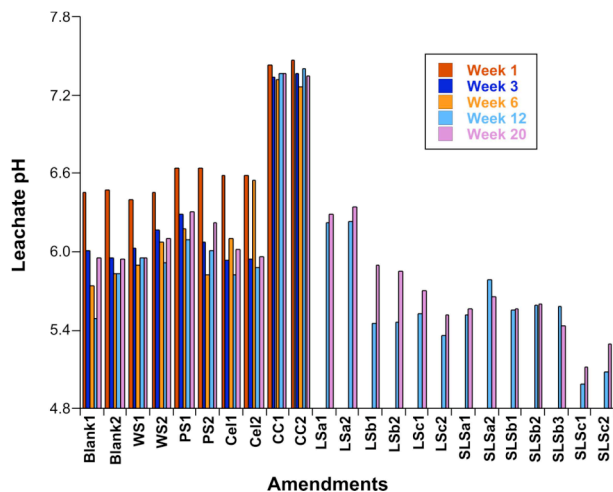


Figure 11. Time courses of leachate pH from ageing of PRL60 soil amended with none (Blank), wheat straw (WS), pine shaving (PS), lignosulfonate (LS), sugared lignosulfonate (SLS), cellulose (Cel), or CaCO_3 (CC). a-c are 0.5%, 1%, and 1.5% of LS or SLS, respectively. Other organic amendments are at 1% while CC is at 0.5%. The 1% SLS amendment was triplicated while the rest were duplicated.

In these experiments, LS and SLS were applied as powder, which led to a significant loss of the amended material via leaching, as evident from their UV-Vis signatures in the leachates (data not shown). The leached LS and SLS were accompanied by a much enhanced metal leaching (relative to the blank treatment) as illustrated in Figure 12 for Pb (cf. Week 8 data). A similar trend was also evident for Cr, V, Cu, and Ag. This increased mobilization of metals correlated with the amount of LS or SLS applied, which may reflect the binding capacity of lignosulfonates for these metals. It may also be related to the soil acidification observed for the LS and SLS treatments (Figure 11). A similar observation was also made for a parallel set of ageing experiments conducted with another Cd-contaminated McClellan soil (A6) (data not shown).

Based on these results, subsequent ageing experiments were conducted by applying a reduced amount of LS and SLS (0.25%, w/w) and as solution to enhance their adsorption to the mineral matrix. In addition, all organic amendments were applied together with 0.5% CaCO_3 to help maintain a neutral pH. Inclusion of CaCO_3 along with the organic amendments prevented the soil acidification, with all leachate pH's remained above neutral throughout the 5-month ageing period (data not shown). Applying LS and SLS in solution forms also minimized their initial leaching from the soil column (data not shown). These measures had a profound impact on the metal leaching profiles, as shown in Figure 13, where the total amounts of metals leached over 5 months were plotted as a function of the treatment. It is clear that the excessive leaching of Pb, Cr, and Cu was eliminated by the modified approach (cf. Figs 3 and 4). It is also evident that CaCO_3 (CC) treatment alone dramatically reduced the amount of transition metals, Cd and Cr leached from the soil. This could be related to the maintenance of soil pH near neutral.

However, CaCO_3 did not prevent Pb leaching while enhancing the release of Ba (data not shown). Also noted was an additive effect of cellulose (Cel) amendment on reducing the leaching of the transition metals and Cd.

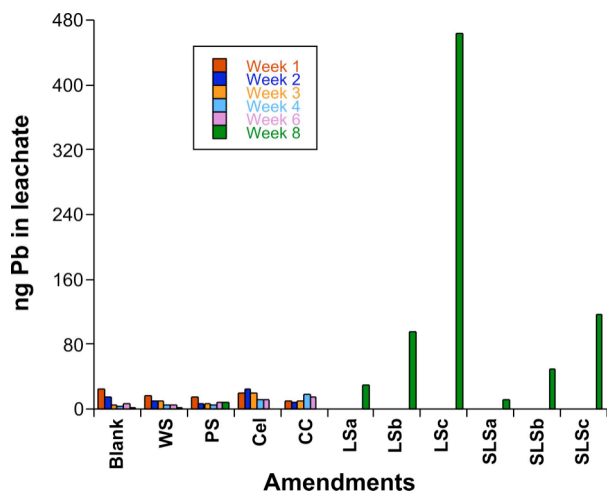


Figure 12. The Pb leaching time courses for the ageing experiments described in Figure 11. Leachate collection started on Week 1 for the Blank, WS, PS, Cel, and CC treatments while that for the LS and SLS treatments began on Week 8 to allow the amendment to interact with the soil matrix.

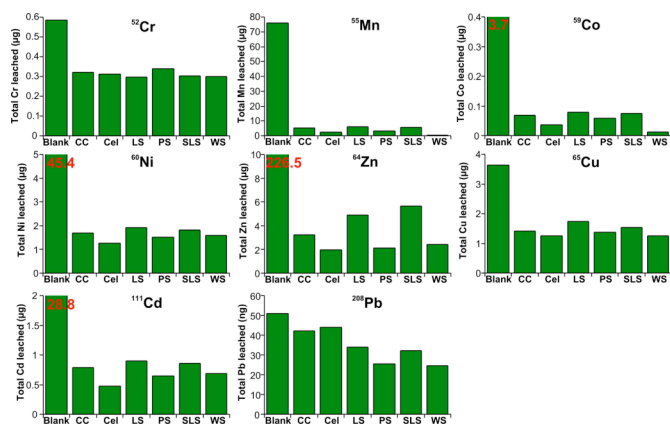


Figure 13. Total metal profiles of leachates from the 2nd ageing experiment. The values for Co, Ni, Zn, and Cd were plotted off-scale and are listed in red.

IV.C.2. Ageing of ¹³C Labeled Soils

To investigate the chemical mechanism of the amendment effect, the PRL 60 soil was labeled with ¹³C by incubating the soil with ¹³C-glucose for 8 months. The prelabeled soil was then amended with CaCO_3 plus unlabeled organic matters and incubated for 7 more months. The 1st leachate was collected after 1 month of incubation and a total of 6 leachates were obtained.

Again, the leachate pH in this labeled experiment remained above or near neutral for all but the blank treatment which acidified to as low as pH 5.3 after 7 months. The time course changes of transition metals, Cd, and Pb for the ¹³C labeled experiment are shown in Figure 14. Other parallel labeled experiments exhibited a qualitatively similar trend as that in Figure 14. The blank treatment with no amendment contained the highest amounts of metals in all leachate collections, except for Mn. In contrast, the cellulose treatment had the lowest metal content in most leachate collections. The leachate time course for Pb differed from those of the other metals, showing a large increase after the 4th collection for all treatments. □ □ This increase was most pronounced for the CaCO_3 only treatment, which is consistent with the observation for the unlabeled 2nd ageing experiment. Displacement of bound Pb by Ca may underlie this behavior.

In addition, the Pb time courses here differed from those of the 2nd ageing experiment (Figure 13 and data not shown) which did not show a “breakthrough” of Pb. This difference may be due to the longer length of incubation (7+8 months) and/or added influence of glucose and nitrate.

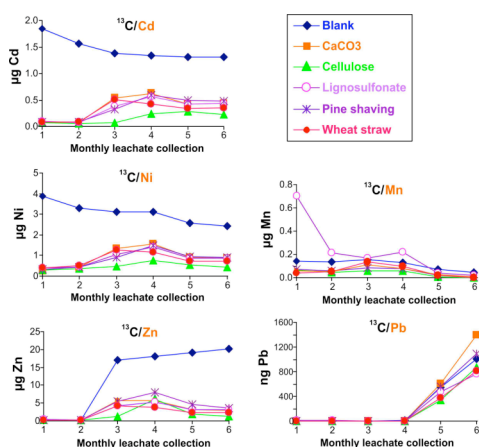


Figure 14. Time courses of metal leaching for the 3rd (¹³C-labeled) ageing experiment. Each treatment was duplicated and all data points were an average of the duplicates.

IV.C.3. 3-D Fluorescence Analysis of Humified Products

The mobile HS (mHS) isolated from the 2nd ageing experiment was subjected to 3-D fluorescence analysis both in the absence and presence of CdSO₄. Distinct changes in the 3-D spectrum in all mHS samples were observed upon addition of Cd, where emission spectral changes were most significant with excitation wavelengths of 260 to 280 nm. Example emission spectra of two mHS preparations as a function of Cd concentrations are shown in Figure 15. Decreases in fluorescence intensity were evident in both sets of spectra with maximal changes centered about 400 nm. The intensity changes followed a non-linear function of the added Cd concentrations, reaching a plateau value at 0.2 mM Cd. A further decrease in intensity was noted after 3 days of mHS interaction with Cd, as illustrated for the WS treated sample. Altogether, these results suggest that the Cd-induced fluorescence changes of mHS resulted from Cd binding and that this binding may lead to a rapid and a slower conformational change in the HS.

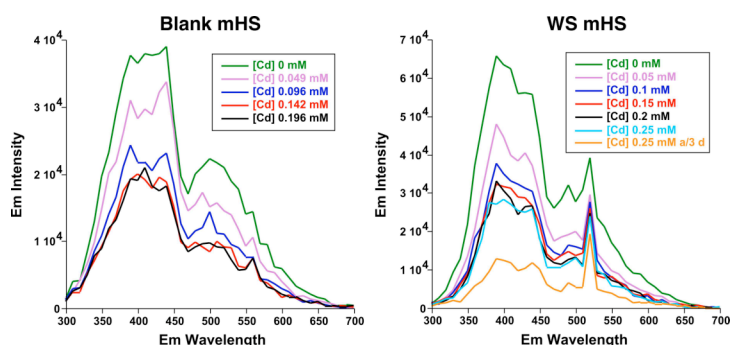


Figure 15. Fluorescence emission spectra of blank and WS-treated mHS isolated from the 2nd Ageing experiment. The excitation wavelengths for the blank and WS spectra were 280 and 260 nm, respectively. CdSO₄ was added sequentially to mHS to the specified concentrations. For the WS-treated mHS, spectrum was also taken after 3 days of incubation with Cd at room temperature.

IV.C.4. NMR Analysis of Humified Products

The ¹H NMR spectra were acquired at 18.8 T to maximize the spectral resolution. Figure 16 illustrates the 1-D spectra for all 6 treatments of the ¹³C-prelabeled soil. All spectra were scaled for direct comparison of peak intensity, which reflected the abundance of individual substructures of mHS. The assignment of these substructures was made based on the 2-D ¹H TOCSY (cf. Figure 17) and ¹H-¹³C HSQC spectra (cf. Figure 18) described below. As expected,

the aromatic/phenolic structures in the mHS of LS, PS, and WS were more abundant relative to those in the mHS of blank, CC, and Cel, since the former group of amendments is rich in lignins or phenolics. The abundance of peptidic alanine (A), valine (V), leucine (L), and isoleucine (I) was somewhat attenuated in the mHS of Cel and WS treatments, which may be related to their faster turnover (see result below). It is also interesting to note the substantial increase in the intensity of a sharp peak near 0 ppm for the LS and PS treatments. This peak most likely arose from an organosilicon group, which has been observed in the ^1H NMR spectra of other HS preparations (Fan et al., 2000).

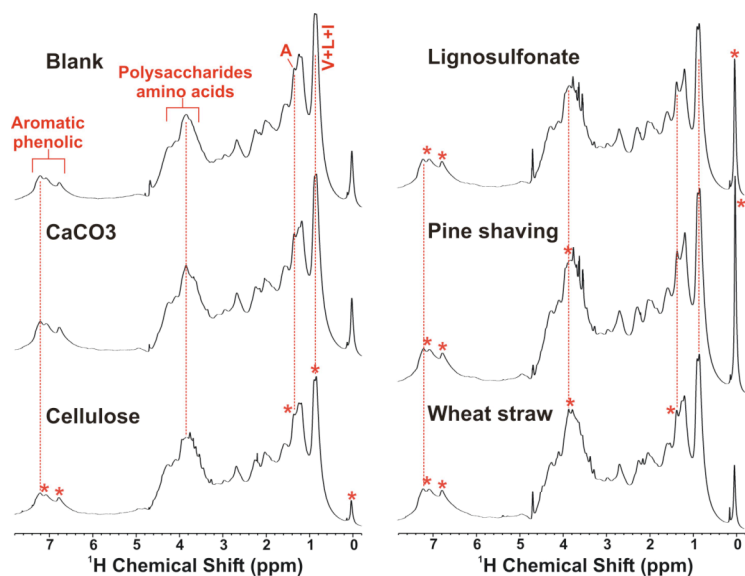


Figure 16. 1-D ^1H NMR spectra of mobile HS extracted from aged PRL60 soil pre-labeled with ^{13}C -glucose. The NMR spectra were acquired at 18.8 T and 30°C. The peak intensity of all spectra was normalized to that of the cellulose treatment for comparison. The * denotes a difference in ^1H abundance for the amended HS from that for the blank HS, e.g. an increase in the aromatic/phenolic noted for the LS, PS, and WS HS while a decrease evident for the CaCO₃ HS.

To obtain detailed chemical assignment for the 1-D ^1H NMR spectra, 2-D TOCSY spectra were acquired on the same set of mHS samples. Figure 17 illustrates the TOCSY spectrum of the mHS for the PS treatment. The ^1H covalent linkages, as represented by off-diagonal cross-peaks, were traced by the rectangular boxes. This, together with the chemical shift information, allowed the assignment of various peptidic amino acid residues and structural components of nucleic acids such as the deoxyribose and pyrimidine ring residues. As noted previously (Fan et al., 2000; Fan et al., 2004), the TOCSY spectrum was dominated by the covalent linkages (cross-peaks) of peptidic amino acids while those for the polysaccharides were absent. Based on the chemical shift and py-GC-MS data (see below), polysaccharidic structures were present in all mHS samples. This lack of covalent linkage signatures may reflect a restricted molecular environment for the saccharides in the HS.

To verify and complement the ^1H NMR assignment, 2-D ^1H - ^{13}C HSQC experiments were performed on the same set of mHS samples as in Figure 16. Two example HSQC spectra are shown in Figure 18, where the spectra of the blank and Cel-CC-amended mHS are compared. The ^1H - ^{13}C covalent linkages (expressed as cross-peaks) confirmed the peptidic assignment made in Figure 17 while revealing the assignment for polysaccharides, alkenes, and methoxy groups from lignaceous structures. In addition, the peak intensity in the 1-D ^{13}C projection spectra (Figure 19) indicates the relative abundance of ^{13}C label in each chemical group. By comparing spectra A and C, it is clear that most, if not all, of the chemical groups in the Cel-CC amended mHS were much lower in ^{13}C abundance than those in the blank treatment. This

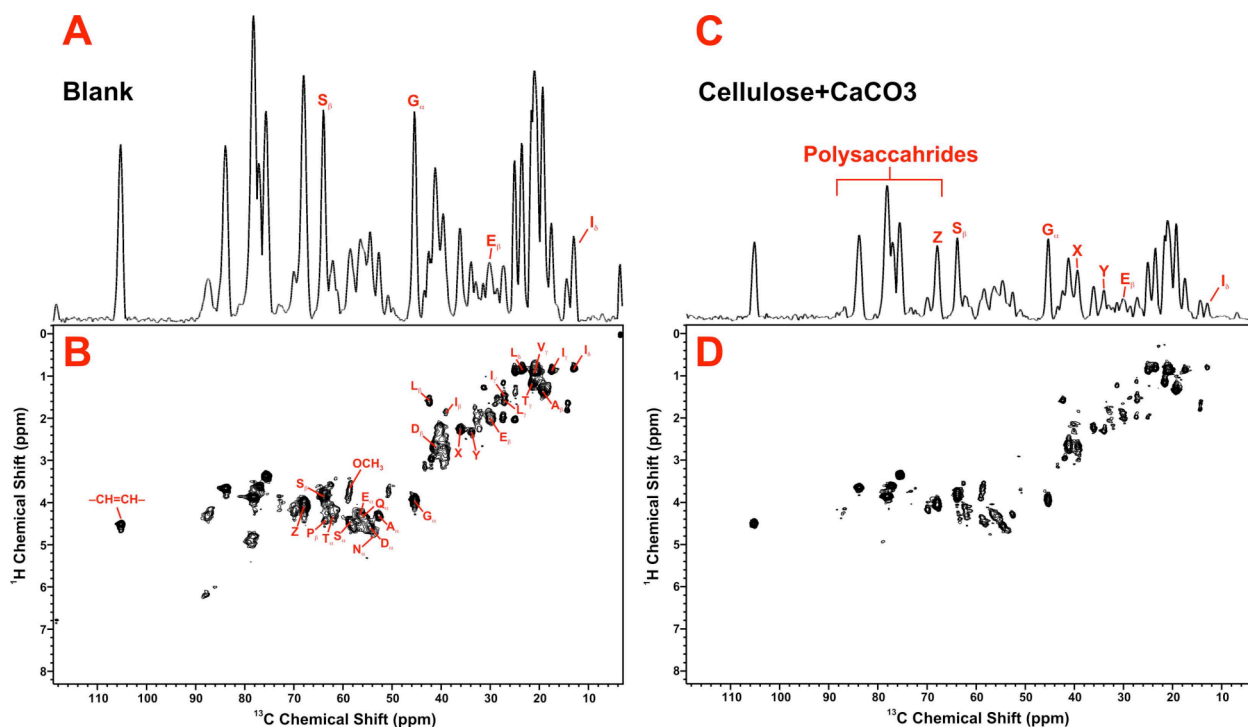


Figure 18. 2-D ^{13}C - ^1H HSQC NMR spectra (B,D) are shown with the corresponding 1-D ^{13}C projection spectra (A,C) of mobile HS (mHS) isolated from ^{13}C labeled PRL60 soils amended with none (blank) or with cellulose+ CaCO_3 (Ce-CC). The HSQC spectra allowed ^{13}C -enriched peptidic substructures of mHS to be discerned while the peak intensity of the 1-D projections compared the ^{13}C abundance between the two treatments. Relative to the blank, the Ce-CC treatment shows an overall large decrease in the ^{13}C abundance of various peptidic residues, which indicate a faster turnover of these carbons in the latter treatment. A differential turnover of peptidic glutamate ($\text{E}\beta$), isoleucine ($\text{I}\delta$), glycine ($\text{G}\beta$), and serine ($\text{S}\beta$) relative to other humic carbons was also observed for the Ce-CC-treated soil (cf. \AA & B). X, Y, Z denotes unassigned peaks. Polysaccharidic and alkenic peaks were tentatively assigned based on the ^1H and ^{13}C chemical shifts.

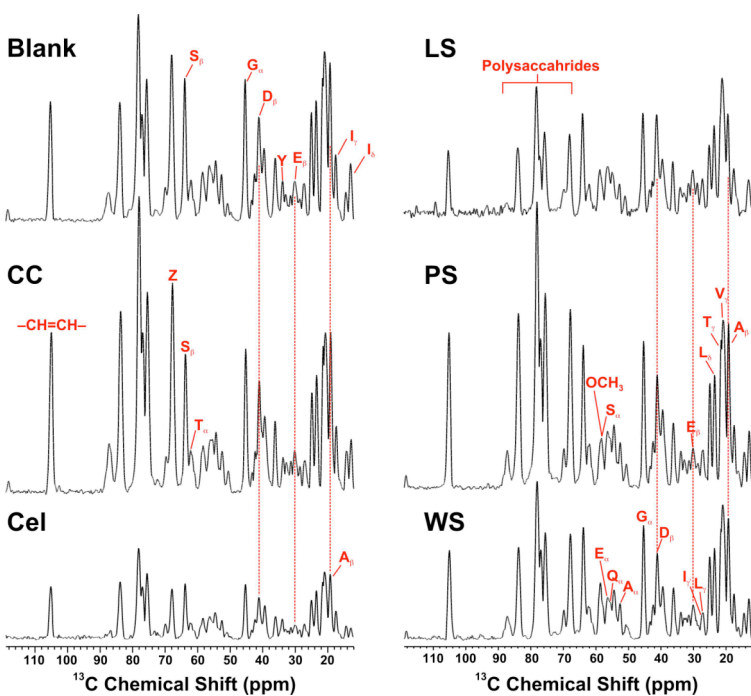


Figure 19. ^{13}C HSQC projection spectra of mobile HS extracted from ^{13}C -prelabeled PRL60 soil aged in various amendments. Acronyms are as defined in Materials & Methods. Cel, LS, PS, and WS amendments also contained CaCO_3 (CC). The peak intensity reflects ^{13}C abundance of various humic substructures, of which many were assigned to peptidic amino acids (cf. Figure 18). The OCH_3 group assigned is likely to arise from lignaceous structures.

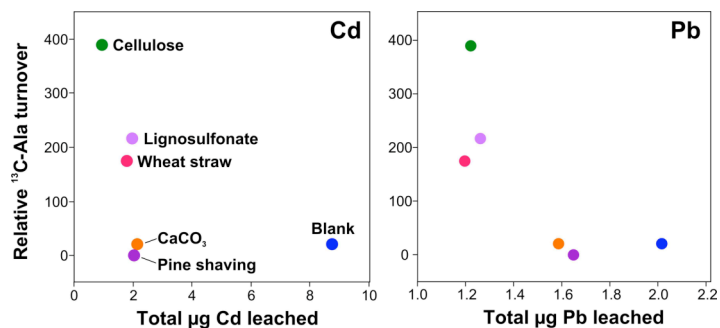


Figure 20. mHS turnover versus total Cd leached from ¹³C-labeled PRL60 soils aged as in Figure 18. mHS turnover is represented by the reduction in ¹³C peak intensity of the peptidic alanine (A_β) for the amended mHS relative to the blank mHS, as measured from Figure 19.

IV.C.5. Pyro-GCMS Studies of HS Turnover and Abundance

The peptidic alanine turnover described above may reflect the fate of selected substructure(s) of mHS, which could differ from the fate of other parts of mHS. To examine the general turnover property of organic matter in the 3rd ageing experiment, pyro-GCMS analysis was employed.

As with NMR, pyro-GCMS is capable of detecting ¹³C and ¹⁵N labels in various structure components of SOM, in particular HS. Thus, the humification kinetics of different OM structure components may be discerned by these techniques. For its part, pyro-GCMS analysis typically yields hundreds of thermolytic-mass fragments that are derived from various components of SOM including lignaceous, cellulosic, proteinaceous, polysaccharidic, long-chain alkanes, etc. The sheer complexity of the data yields a richness of pattern unique for a given soil or OM. Such “chemical fingerprinting” capability offers an excellent opportunity for a comprehensive chemical profiling of SOM and its isolated HS, from which isotopic enrichment of a given chemical group can also be quantified. Despite its capability of producing extremely detailed data on HS, chemical reactions can occur during thermolysis, which precludes reliance on pyro-GCMS alone for structure analysis of complex HS. When coupled with NMR, which provides structure information on intact SOM, a detailed, yet more reliable structure characterization of HS can be achieved (Fan et al., 2000).

This specific strategy of relating detailed HS structures to metal leaching has been successful in soils from the DOE Savannah River Site (Higashi et al., in press), described in section IV.B. In that study – as with this study - we used a combination of NMR and pyro-GCMS analyses to determine the residual ¹³C labeling of HS substructures, which revealed that turnover—not the abundance *per se*—of polysaccharidic and lignic HS substructures was associated with reduced leaching of Cd, Ni, and Cs.

To gain an overview profile of the organic matter, whole soil was first analyzed by pyro-GCMS. The main advantage of directly analyzing whole soils is minimal sample preparation, which can help avoid unexpected chemical alterations during HS extraction. However, there are disadvantages, of which the major ones are the unavoidable inclusion of live microbial biomass, and possible alteration of result because of cross-reaction with inorganic materials. These disadvantages are largely alleviated by analyzing the extracted HS (as with the NMR), which is described in the section following this one.

Pyro-GCMS analysis of the whole soil revealed several interesting results. First, the incorporation of isotope in both ¹³C and ¹⁵N experiments were clear in most peaks by pyro-GCMS analysis, indicating extensive incorporation of the isotopes into a wide range of SOM constituents. Secondly, examination of a peak (methyl indole) representing the peptide bond structure showed two distinct pools of peptidic materials for the ¹³C experiment, those with all carbons labeled and those with no carbons labeled. The interpretation of the pyro-GCMS pattern

was explained earlier in Figure 6. This indicates that partial carbon incorporation into peptide bonds was negligible under these conditions, such that incorporation of glucose carbons into peptides was an all-or-none process. This also indicates that, after many weeks, there remains a pool of peptidic material that does not turn over in this system. This is consistent with our earlier finding of a considerable pool of peptidic material remaining in natural soil humics (Fan et al., 2000; Fan et al., 2004), contrary to the “old school” assumptions, based on no direct evidence, that peptidic material will be rapidly turned over in soil.

Overall, the pyro-GCMS analysis revealed a plethora of detailed changes in the organic matter over the course of the experiment. Figure 21 shows the trends that were observed between % Turnover and Abundance across the various treatments (Blank, CaCO₃, WS, PS, Cel, and LS). It is interesting to note that the turnover of soil lignic structures varied widely while their abundance changed little across different treatments. The opposite was observed for peptidic and polysaccharidic structures.

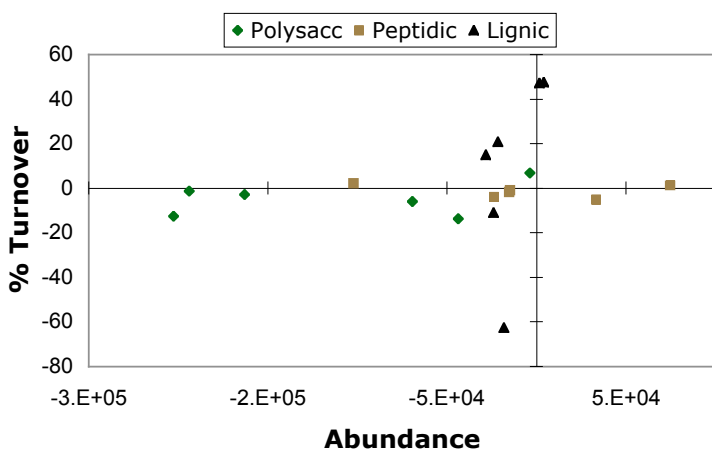


Figure 21. Relationship between % turnover and abundance in whole soils as measured by pyro-GCMS. As shown here, the different treatments (Blank, CaCO₃, WS, PS, Cel, and LS) with natural bulk materials successfully created a wide range of responses in the different ‘chemistries’ of HS. Each datum is a treatment (labels omitted for clarity). In summary, the Polysaccharidic (green diamonds) and Peptidic (brown square) structures varied primarily in Abundance among treatments, while Lignic (black triangle) structures varied mostly in the % Turnover axis.

The pyro-GCMS data was further examined by plotting Turnover and Abundance of the three constituents against the total amount of Cd leached during the experiment. Figure 22 shows the two parameters that appeared to relate to Cd leaching. Taken together, the NMR and pyro-GCMS evidence suggests that, for peptidic structures, both Turnover and Abundance may be important for reduced leaching. Unlike NMR, differences in protein Turnover were too small to be measured effectively by pyro-GCMS. Therefore, pyro-GCMS was not able to immediately confirm the NMR findings; instead the technique contributed complementary information.

To compare with the NMR results of Turnover, and to avoid the potential problems with analyzing whole soils by pyro-GCMS (see preceding section), the very same mHS samples analyzed by NMR were also subjected to pyro-GCMS analysis. Figure 23 reveals that the relationships between Turnover and Abundance seen from direct analysis of whole soils (Figure 21) did not hold for the lignic or peptidic structures of mHS. Contribution of organic matter other than mHS to whole soils could underlie this difference.

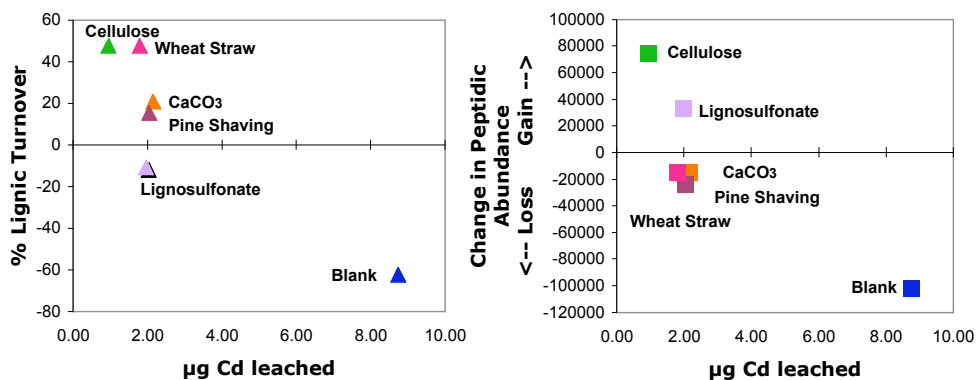


Figure 22. Relationships between Turnover or Abundance vs. Cd leaching, as measured by pyro-GCMS analysis of whole soil. Left panel: Pyro-GCMS revealed that Lignin structures Turnover displayed a possible sigmoidal function with Cd leaching. As with the NMR data, the cellulose and blank treatments showed clear opposing trends. Right panel: There was also a relationship of Cd leaching with the changes in Peptidic Abundance over the course of the experiment. It is possible that this is also a sigmoidal function.

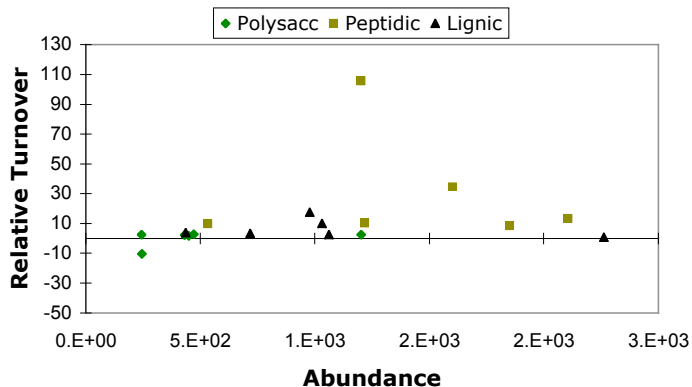


Figure 23. Relationship between turnover and abundance in mHS as measured by pyro-GCMS. This figure is comparable to Figure 21, except that mHS was analyzed. Each datum is a treatment (labels omitted for clarity). In summary, the relationship between turnover and abundance of the lignin and peptidic structures observed for whole soils (Figure 21) did not hold for mHS - Polysaccharidic (green diamonds), Peptidic (brown square), and Lignic (black triangle).

Once again, we compared both Turnover and Abundance across all treatments for each of the mHS constituents (polysaccharidic, peptidic, lignic), with Cd leaching. Figure 24 shows the correlation of Turnover of lignin and peptidic constituents in mHS with Cd leaching. None of the others compared showed a trend, e.g. the peptidic abundance relation to Cd leaching (Figure 21) did not hold. As mentioned above, this difference in trend between whole soils and mHS could be due to the complication from other organic materials such as microbial biomass in whole soils.

The lignin Turnover relationship to Cd leaching (Figure 24, left) appeared to be similar to that observed from pyro-GCMS analysis of whole soils (Figure 22), while the peptidic Turnover relationship (Figure 24, right) bore some similarity to the results from NMR analyses (Figure 20). It should be noted that the NMR turnover analysis was based on the specific alanine residue while the pyro-GCMS analysis was derived from the peptide structures of many different residues. The similarity or difference between the two analyses could reflect a similar or differential turnover between alanine and other amino acid residues, as noted in Figure 19.

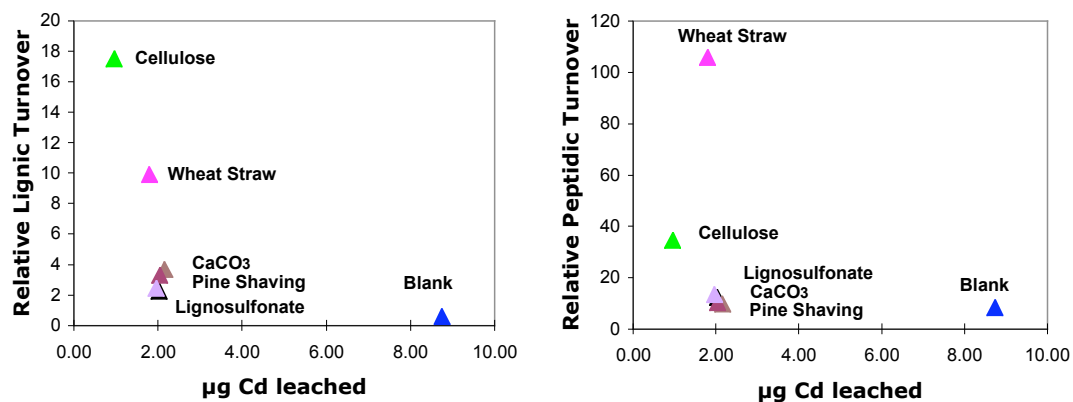


Figure 24. Relationships between Turnover of mHS vs. Cd leaching, as measured by pyro-GCMS. Left panel: Pyro-GCMS revealed that Lignic structures Turnover related to Cd leaching, a relationship similar to that from analysis of whole soil. Right panel: Also observed was a relationship of Cd leaching with the changes in Peptidic Turnover over the course of the experiment, a result comparable to that from NMR analyses (Figure 20).

V. Summary and Conclusions

These studies demonstrated the utility of amendment with natural bulk materials for reducing metal leaching in contaminated DOE site and military base soils. The combination of ageing experiments, isotopic enrichment, and structure/dynamic characterization provided molecular-level information on humification processes in relation to metal mobility and binding that has eluded scientific inquiries in the past. The advanced approach showed that the manipulation of the metal leaching behavior with amendment was due to turnover of lignocellulosic components of soil humic substances.

The findings are consistent with recent literature regarding the role of SOM as metal sink while contrast to the general belief in the degradability of peptides in soil humics. In addition, the present study brings up several issues that are useful to explore in the context of sustainable and holistic metal remediation:

- Can a wide range of toxic metals be immobilized with different combinations of chemically diverse organic and inorganic amendments?
- What is the long-term fate and bioavailability of the immobilized metals?
- Are similar chemical mechanism(s) operating in different soil types?
- Can a general set of guidelines be established for immobilizing metals in a diverse range of soils?

The fulfillment of these questions can lead to an *in situ* bioremediation scheme that has the following advantages:

- readily deployable in most cases
- highly economical with low startup and maintenance costs
- long-term sustainability
- less, if not the least, perturbing to soil ecosystems
- possibly already “deployed”, e.g. in SRS Managed Natural Attenuation sites.

Acknowledgements

This work was supported by DOE Environmental Science Management Program, grant # DE-FG07-96ER20255.

Peer-reviewed Publications Credited to this Grant

- Baraud, F., T. W. M. Fan, et al. (manuscript accepted). Interactive effect of cadmium and soil humates on metal acquisition and sequestration in wheat. Environmental Chemistry. R. D., European Association of Chemistry and the Environment, Springer.
- Fan, T.W-M., Baraud, F., Higashi, R.M. (2000). Genotypic influence on metal ion mobilization and sequestration via metal ion ligand production by wheat. In: Nuclear Site Remediation. Washington, D.C., American Chemical Society Symposium Series, vol. 778, pp. 417-431.
- Fan, T.W-M., Higashi, R.M., Lane, A.N. (2000). Chemical Characterization of a Chelator-Treated Soil Humate by Solution-State Multinuclear Two-Dimensional NMR with FTIR and Pyrolysis-GCMS. Environ. Sci. Technol. 34(9): 1636-1646.
- Fan, T.W-M., A.N. Lane, J. Pedler, D. Crowley, and R.M. Higashi (1997). Comprehensive analysis of organic ligands in whole root exudates using nuclear magnetic resonance and gas chromatography-mass spectrometry. Analytical Biochemistry 251(1): 57-68
- Fan, T.W-M., Lane, A.N., Shenker, M., Bartley, J.P., Crowley, D., Higashi, R.M. (2001) Comprehensive chemical profiling of gramineous plant root exudates using high-resolution NMR and MS. Phytochemistry 57: 209-221.
- Fan, T.W-M., Lane, A.N., and Higashi, R.M. (2004) An electrophoretic profiling method for thiol-rich phytochelatins and metallothioneins, Phytochemical Anal. 15: 175-183.
- Fan, T.W-M., Lane, A.L., Chekmenev, E., Wittebort, R.J., Higashi, R.M. (2004) Synthesis and Physico-Chemical Properties of Peptides in Soil Humic Substances, Journal of Peptide Research 63: 1-12.
- Higashi, R.M., Cassel, T.A., Green, P.G., Fan T.W-M. (In Press) ¹³C-tracer studies of soil humic substructures that reduce heavy metal leaching, In: Subsurface Contamination Remediation: Accomplishments of the Environmental Management Science Program, T. Zachary and E. Berkey (eds.), American Chemical Society Symposium Series, in press.
- Higashi, R.M., T. W-M. Fan, and A.N. Lane. (1998) Association of deferrioxamine with humic substances and their interaction with cadmium(II) as studied by pyrolysis-gas chromatography-mass spectrometry and nuclear magnetic resonance spectroscopy. The Analyst, 123: 911-918.
- Shenker, M., T. W. M. Fan, et al. (2001). "Phytosiderophores influence on cadmium mobilization and uptake by wheat and barley plants." Journal of Environmental Quality 30(6): 2091-2098.

References Cited

- Baraud, F., T. W. M. Fan, et al. (manuscript accepted). Interactive effect of cadmium and soil humates on metal acquisition and sequestration in wheat. Environmental Chemistry. R. D., European Association of Chemistry and the Environment, Springer.
- Bundy, L. G.; Meisinger, J. J. (1994) Nitrogen Availability Indices. In: Methods of Soil Analysis; Weaver, R. W., Ed.; Soil Science Society of America Book Series No. 5; SSSA: Madison, WI.
- Clark, R. B., V. Römheld, et al. (1988). "Iron uptake and phytosiderophore release by roots of Sorghum genotypes." Journal of Plant Nutrition 11(6-11): 663-676.

- Fan, T. W.-M., F. Baraud, et al. (2000). Genotypic influence on metal ion mobilization and sequestration via metal ion ligand production by wheat. In: Nuclear Site Remediation. Washington, D.C., American Chemical Society Symposium Series, vol. 778, pp. 417-431.
- Fan, T. W.-M., R. M. Higashi, et al. (2000). "Chemical Characterization of a Chelator-Treated Soil Humate by Solution-State Multinuclear Two-Dimensional NMR with FTIR and Pyrolysis-GCMS." Environ. Sci. Technol. **34**(9): 1636-1646.
- Fan, T. W. M., A. N. Lane, et al. (1997). "Comprehensive analysis of organic ligands in whole root exudates using nuclear magnetic resonance and gas chromatography-mass spectrometry." Analytical Biochemistry **251**(1): 57-68.
- Fan, T. W. M., A. N. Lane, et al. (2001). "Comprehensive chemical profiling of gramineous plant root exudates using high-resolution NMR and MS." Phytochemistry (Oxford) **57**(2): 209-221.
- Fan, T.W-M., Lane, A.L., Chekmenev, E., Wittebort, R.J., Higashi, R.M. (2004) Synthesis and Physico-Chemical Properties of Peptides in Soil Humic Substances, Journal of Peptide Research **63**: 1-12.
- Higashi, R.M., Cassel, T.A., Green, P.G., Fan T.W-M. (In Press) ¹³C-tracer studies of soil humic substructures that reduce heavy metal leaching, In: Subsurface Contamination Remediation: Accomplishments of the Environmental Management Science Program, T.Zachary and E. Berkey (eds.), American Chemical Society Symposium Series, in press.
- Higashi, R. M., T. W. M. Fan, et al. (1998). "Association of desferrioxamine with humic substances and their interaction with cadmium(II) as studied by pyrolysis gas chromatography mass spectrometry and nuclear magnetic resonance spectroscopy." Analyst **123**(5): 911-918.
- Kinnersley, A. M. (1993). "The role of phytochelates in plant growth and productivity." Plant Growth Regulation **12**(3): 207-218.
- Marschner, H. (1995). Mineral nutrition of higher plants. London ; San Diego, Academic Press.
- Olk, D. C., K. G. Cassman, et al. (1995). "Characterization of two humic acid fractions from a calcareous vermiculitic soil: Implications for the humification process." Geoderma **65**(3-4): 195-208.
- Schultz L.F., Young T.M., Higashi R.M. (1999) Sorption-desorption behavior of phenanthrene elucidated by pyrolysis GCMS studies of soil organic matter. Environmental Toxicology and Chemistry, **18**:1710-1719.
- Shenker, M., T. W. M. Fan, et al. (2001). "Phytosiderophores influence on cadmium mobilization and uptake by wheat and barley plants." Journal of Environmental Quality **30**(6): 2091-2098.
- Strickland, R. C., W. R. Chaney, et al. (1979). "Organic-Matter Influences Phytotoxicity of Cadmium to Soybeans." Plant and Soil **52**(3): 393-402.